Biomechanical Design, Modeling and Control of an Ankle-Exosuit System

Liugang Zhao, Sen Huang, Yiyou Li, Xinzhili Chen, Dong Yuan, Minchao Liu, Jiahong Liu, Xiaodong Qin, Han Cui, and Bo Li(✉)

Chongqing University of Technology, Chongqing 400000, NJ, China
libo_doctor@163.com

Abstract. To improve the walking abilities of the ankle patients with locomotion impairment, a biomimetic Ankle-Exosuit was designed based on the muscle-tendon-ligament model. The Ankle-Exosuit assisted ankle plantarflexion by exerting a force parallel to the muscle to reduce plantar flexor activation and enhance lower extremity walking endurance. The bandage locomotion could be effectively reduced by the designed lacing mechanism. We established the coupled kinematic model of human-exosuit. To determine the opening and closing times of the ankle plantarflexion assistance, a threshold detection algorithm was proposed for the recognition of heel-off (HO) and toe-off (TO). A trajectory generator according to the fusion of the coupled kinematic model and trajectory generation function was developed. Comparison experiments based on the measurements of the surface electromyographic (sEMG) signals demonstrated that when wearing the Ankle-Exosuit, the locomotion activation of the gastrocnemius muscles (GM) and soleus muscles (SM) decreased by 11.09% and 6.5%, respectively. The proposed Ankle-Exosuit can decrease muscle fatigue to achieve effective walking assistance.

Keywords: Ankle-Exosuit · Gait recognition · Coupled kinematic model · Trajectory generator

1 Introduction

The ankle plays an imperative part in walking and running activities. However, gait abnormalities [1], and muscular weakness [2], are prevalent problems in ankle locomotion impaired patients. Lower extremity exoskeleton that augments ankle locomotion performance and decreases muscle activation has continuously attracted investigation.

Lower extremity exoskeleton can be divided into rigid and soft exoskeleton. In the previous research, most of these assistive devices are active rigid lower extremity exoskeletons [3]. HAL, [4] ReWalk, [5] and Ekso GT™ [6], are typical rigid lower extremity exoskeletons. These rigid exoskeletons implement human-exoskeleton locomotion couple by rigid link mechanism and assist mobility by directly drive. However, the rigid link mechanism and powerful motors dominate the gait of the wearer, it enforces the walking pattern, results in limited movement flexibility. In contrast to rigid lower extremity exoskeleton, the soft lower extremity exoskeleton is characterized by compact size, lightweight, and locomotion flexibility [7].

H. Yang et al. (Eds.): ICIRA 2023, LNAI 14268, pp. 489–502, 2023.
https://doi.org/10.1007/978-981-99-6486-4_42

The research team of Harvard University proposed biological muscle-tendon-ligament model [8], and virtual anchor technique [9], to design flexible lower extremity exoskeleton. Their model and technique provided inspirations for the design of the Exo-Suit [10], Myosuit [11], etc. However, because to the presence of shear pressures in the assistance process, problems like as bandage locomotion and assistance lag arise, which must be addressed. In addition, the human-exosuit control system is another key technology that need to be considered.

Ding, et al. [12] used a control strategy of iterative learning to update the position profile of the actuator, which provided assistance by controlling the start time, peak time and peak size of the control force. Harvard University enhanced accuracy of the aided trajectory tracking by using a force-position hybrid control technique [10] and a guide position controller [13]. The above controls were designed mainly according to human-exosuit interaction information, which did not consider human-exosuit coupling kinematic and kinetic. The development of flexible lower extremity exoskeleton needs to consider not only control performance but also the entire human-exosuit system [14].

To solve the above problems, we developed an Ankle-Exosuit based on the muscle-tendon-ligament model, designed a trajectory generator according to the coupled kinematic model of human-exosuit and threshold detection algorithm to achieve effective walking assistance.

2 Ankle-Exosuit Mechanism Design

2.1 Biomechanics of Ankle Locomotion

This section introduced the biological principles of ankle locomotion, which was an important guidance for the biomimetic design of the Ankle-Exosuit and the surface electromyographic (sEMG) experiments.

The soleus muscles (SM) and gastrocnemius muscles (GM) contributed 93% of the plantarflexion moment during natural ankle walking [15]. In contrast, the remaining muscle contributed only 7%. The primary muscle groups contribute to plantarflexion movement of the ankle (Fig. 1), and the total force for these muscle groups can be described by

$$\Sigma F_{ma} = F_{gm} + F_{hm} + F_{others} \tag{1}$$

In the equation, F_{gm} represents the force given by the GM, F_{hm} represents the force produced by the SM, F_{others} represents the sum of the other muscle forces, ΣF_{ma} represents the combined force of the helpful muscle groups. We presumed that the GM and Achilles tendon junction was the floating anchor point $A_r(A_l)$ and the heel subcutaneous capsule mimic was the fixed anchor point $B_r(B_l)$. We imitated the morphology and function of biological muscle-tendon-ligament structures by using the Bowden cable. The typical length of the Achilles tendon in adult males is around 15 cm, and the Bowden cable was initially set at 18 cm to accommodate displacement error. We indirectly provided a portion of the force in the form of a Bowden cable.

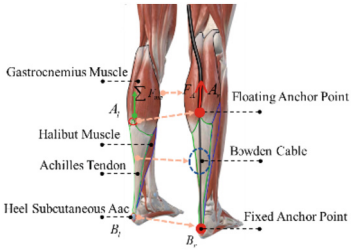

Fig. 1. Biomechanical analysis of ankle locomotion.

2.2 Mechanism Design

The Ankle-Exosuit was developed to assist human locomotion and increase lower extremity walking endurance by reducing muscle activation (Fig. 2), its full mass was approximately 2.5 kg. Two DC servo motors with reducers and servo drivers were positioned at the waist and connected to pulleys, and Bowden cable transmitted torque to the ankles of wearer. Two pairs of plantar pressure sensor insoles measured the force of human-exosuit interaction information while walking and communicated the data to a control board attached to the actuator module with wire. A lithium polymer battery was built into the driver module to power the Ankle-Exosuit.

Human load affects metabolic rate and muscle weariness during walking. In order to reduce the weight of the system, mechanical structure of the Ankle-Exosuit was concentrated on modular, integrated, and lightweight design. Compared with other flexible lower extremity exoskeletons, The Ankle-Exosuit is more flexible to wear, more convenient to carry and less bound movement, which is mainly due to the design and implementation of a rapid tethering mechanism. The driving module and calf strap was designed as follows.

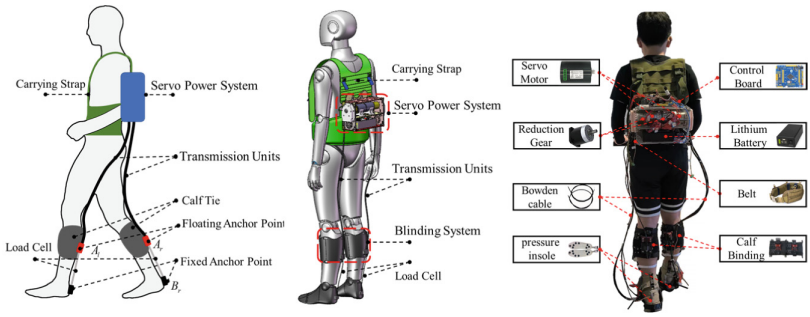

(a) The sketch of the system (b) 3D design of the system (c) Ankle-Exosuit prototype.

Fig. 2. Mechanism design of the Ankle-Exosuit

(1) Actuation design

The Ankle-Exosuit has developed an actuation unit (Fig. 3). To accommodate individualized wear and assistance, we strongly emphasized drive mass and size being

as light and tiny as feasible. The drive assembly was 256 mm long, 168 mm high, and 104 mm broad. The actuation unit includes two DC electric integrated torque servo motors (42AIM30, 0.4 kg) and a planetary gearhead (OKD42PLEK50, 0.35 kg, 50:1 reduction). The motor integrated a 15-bit absolute encoder and servo driver (YZ-AIMD). The system was powered by a lithium battery (44800 mAh, 24 V, 0.41 kg) with its own emergency switch, which can provide nearly 480 min of continuous power to the drive system, which was enough to meet the demand for a more extended range without having to change power sources or recharge midway. The drive system can provide a maximum of 15 NM of extra torque.

The Bowden cable winder comprised a pulley (inner diameter 22 mm, outside diameter 60 mm, thickness 9 mm), a standard bearing (inner diameter 8, outer diameter 14 mm, thickness 4 mm), and support bar (Fig. 3). The Bowden cable sheath was fastened to the end cap of pulley with a cap screw and has an inner diameter of around 1.5 mm and an outer diameter of approximately 5 mm. It was grease-filled to decrease friction and Bowden cable energy transfer loss. The Bowden cable (cable diameter 1.2 mm, load capacity 40.8 kg) was wound on the pulley through the end cover hole, and the Bowden cable head was secured in the pulley groove with double screws, with enough clearance between the end cover and the Bowden cable head to prevent the Bowden cable head from rubbing violently against the end cover.

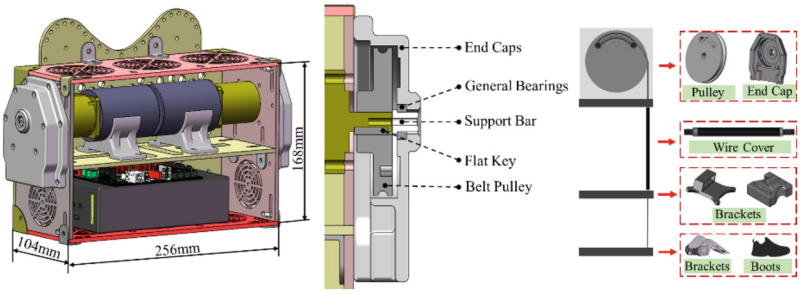

Fig. 3. Drive mechanical design and Bowden cable unit

(2) Flexible bandage design

A functional bandage component for the newly wrapped calf in the Ankle-Exosuit system is shown in Fig. 4. Its total mass was about 0.22 kg. The carrier features a waist belt and a tether strap for simply attaching the actuator to the waist belt. The calf strap has a rapid tethering mechanism to adapt various calf shapes and sizes. The bandage's inner layer, which touches the skin of wearer closely, was constructed of sponges and mesh. The sponge improves comfort and reduces skin abrasion from the bandage, while the mesh's honeycomb surface increases friction between the bandage and the skin. The sponge absorbs perspiration from the calf via the honeycomb pores to prevent slippage under load.

The heel and middle of the shoe contain textile straps linked to the calf bandages to strengthen operating stability of the calf bandages. The far-end of Bowden cable

was linked to a fixed anchor on the heel. Meanwhile, the proximal sheath was attached to a floating anchor on the calf bandage, which was operated by an actuator that compressed the Bowden cable to deliver a mechanical force to the ankle.

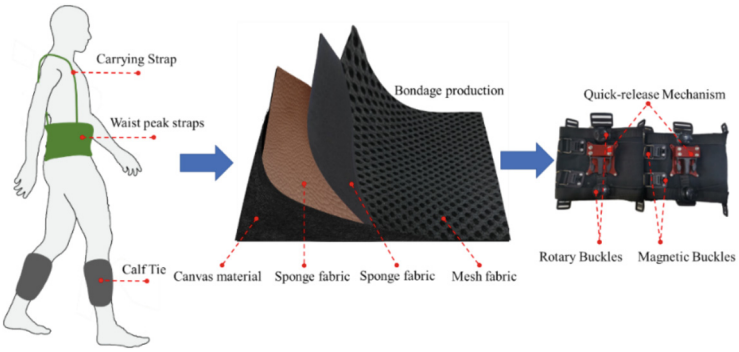

Fig. 4. Flexible bandage design.

3 Human and Ankle-Exosuit Coupled Kinematic

We established a human ankle joint and the Ankle-Exosuit coupling relationship through the lower extremity biokinetic mechanism and derived the ankle joint change angle and motor rotation angle model to support the assistance trajectory generation and tracking of the Ankle-Exosuit.

The geometric link between the angular position of the Ankle-Exosuit pulley q_a and the angular position of the ankle joint θ_a may be represented as depicted in Fig. 5.

$$R_P(q_a - q_{a0}) = r_a(\theta_a - \theta_{a0}) \tag{2}$$

where R_P is the radius of the pulley, q_a is the output angle of the servo motor, q_{a0} is the initial position of the servo motor, r_a is the distance between the center of rotation of the ankle and the fixed anchor of the same heel, θ_a is the plantarflexion angle of the ankle, θ_{a0} is the initial angle of plantarflexion of the ankle joint, $\Delta\theta_a = \theta_a - \theta_{a0}$, $\cdot\theta_1$ is the angle between the initial length of the standing Bowden cable and the foot, that is

$$\theta_1 = arccos\frac{r_c^2 + l_{a1}^2 + r_a^2 - l_{a0}^2}{2r_a\sqrt{r_c^2 + l_{a1}^2}} \tag{3}$$

The ankle plantarflexion locomotion can be simplified to a rotation around the center of rotation. Therefore, the arc traversed by the ankle for the center of rotation was equal to the arc traversed by the pulley. The kinematic model of the ankle joint was obtained by transforming Eq. (2).

$$\theta_a = \frac{R_P}{r_a}(q_a - q_{a0}) + \theta_{a0} \tag{4}$$

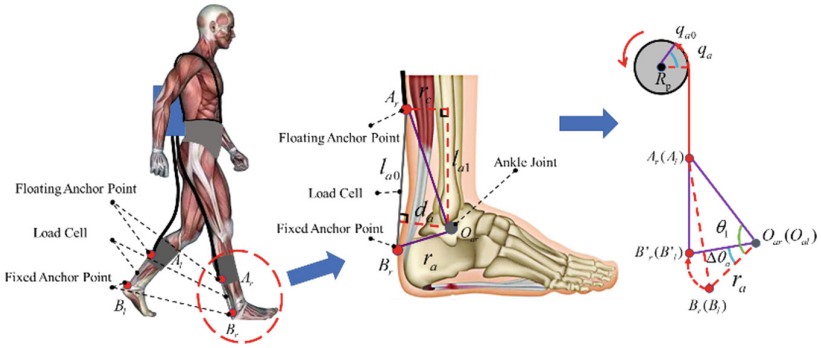

Fig. 5. Coupling relationship between human ankle joint and the Ankle-Exosuit.

4 Gait Recognition

The goal of gait recognition is to aid in decision-making. In this paper, we use a threshold real-time gait phase detection algorithm [16, 17], which detects the mean pressure in the foot-ground contact area using a plantar pressure sensor to achieve heel-off (HO) and toe-off (TO) gait event recognition (see Fig. 6a), with the goal of the controller sending the appropriate assistance start and end commands.

4.1 Gait Analysis

A single gait cycle was separated into seven stages by classifying two contiguous contacts of the ipsilateral heel as an entire cycle, respectively, loading response (LR), middle stance (MSt), terminal stance (TSt), pre-swing (PSw), initial swing (ISt), middle swing (MSw), terminal swing (TSw) (see Fig. 6a). We identified the instant heel strike to the ground as the gait behavior during the weight-bearing response period since it only accounts for roughly 2% of the cycle. The gray region represents the foot pressure recording area, while the orange-red area represents the assistance area. The assistance begins when the heel leaves the ground and finishes when the medial forefoot leaves.

The grey and orange-red areas are the plantarflexion (PF) intervals of the ankle (Fig. 6b), with the grey area muscles passively performing negative work to overcome the energy impact of the environment in order to maintain walking stability and the orange-red area muscles actively performing positive work to change the position and posture of the foot, at this moment, the force exerted by the muscles on the ankle joint is explosive and transient. Practical ankle joint support during active, positive muscular action may minimize muscle fatigue and energy consumption. Therefore, our selection of the orange-red region as the assistance interval is consistent with the biology of lower extremity locomotion.

4.2 Real-Time Gait Detection

A pair of plantar pressure sensors were used to recognize the stride of the HO the ground. Plantar pressure sensors were placed into a boot as a shoe insole, measuring the

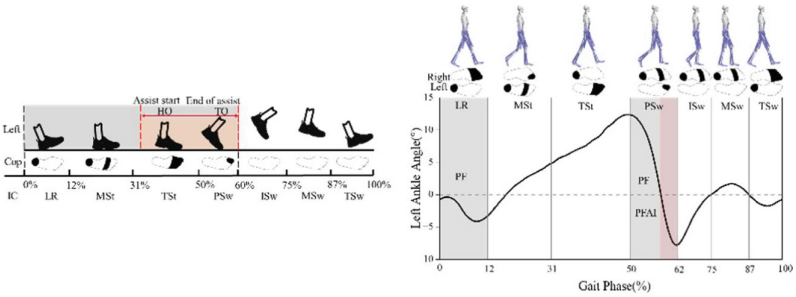

(a) HO and TO gait recognition (b) Plantarflexion assist interval

Fig. 6. Gait analysis of the lower extremity.

contact forces between the foot and the ground. To filter the impact of the environment on the foot pressure measurement, we employed Kalman filtering or complementing filtering methods [18–20] to process the data obtained by the plantar pressure sensors. The microcontroller in the drive unit collected signals from all the sensors by wire. The number and type of sensors was reconfigured to suit different walking experiments and project development requirements.

Each plantar pressure sensor was divided into three areas (Fig. 7), with three pressure points in the forefoot (FF) and pressure values recorded as F_{ff1}, F_{ff2} and F_{ff3}. The middle foot (MF) has two pressure points and the pressure values are noted as F_{ff4} and F_{mf5}. The rear foot (RF) has three pressure points and the pressure values were noted as F_{rf6}, F_{rf7} and F_{rf8}, accounting for 40%, 30% and 30% of the total foot length, respectively [21]. The HO sign was the rapid drop of the pressure signal value in the heel region, and the mean value of the signal in this area must fulfill the following relationship.

$$\begin{cases} \sum_{i=6}^{8} F_{rfi} < 3\varepsilon_r \\ \sum_{i=4}^{5} F_{mfi} < 3\varepsilon_m \\ \sum_{i=1}^{3} F_{ffi} > 3\varepsilon_f \end{cases} \tag{5}$$

where ε_r is the heel strike (HS) detection threshold, ε_m is the foot flat (FF) detection threshold, ε_f is the TO detection threshold. The TO satisfies the following expression:

$$\sum_{i=6}^{8} F_{rfi} + \sum_{i=4}^{5} F_{mfi} + \sum_{i=1}^{3} F_{ffi} < 3\left(\varepsilon_r + \varepsilon_f + \varepsilon_m\right) \tag{6}$$

In order to avoid the influence of the environment and the wearer on the signal acquisition of the plantar pressure sensor, the Ankle-Exosuit conducts a 5-s threshold self-test each time it is powered on. After each gait detection during assistance, threshold updates take place.

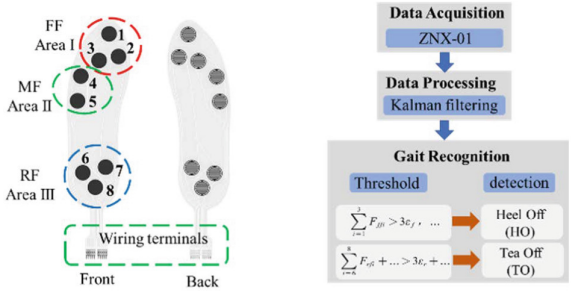

(a) The ZNX-01 (b) Threshold detection algorithm

Fig. 7. Lower extremity locomotion intention recognition

5 Control System Design

Due to the effect of the nonlinear features of the flexible material, the intrinsic characteristics of the drive, and the energy loss of the transmission parts, providing exact help to the wearer at the correct gait phase and the proper assistance interval is a huge issue. In this study, we demonstrated that PID position control, based on the ankle joint kinematic model and overrides locomotion signal input, efficiently guaranteed the precise tracking of the assist trajectory and decreased the additional delay to enhance the stability of human-exosuit cooperative control.

5.1 Controller Design

The Ankle-Exosuit generated auxiliary forces by contracting the Bowden cable, using a PID position controller to change the position of the Bowden cable. We proposed a locomotion control strategy based on a biological model of lower extremity locomotion that can adjust the human gait cycle, amplitude, and contour to suit individualized wearing needs, allowing the assistance trajectory of the position controller to adapt to the natural gait trajectory of human body and enabling active human participation in the assistance. Different from other exosuits control strategies, we emphasized the introduction of the coupling model of human and the Ankle-Exosuit into the control loop, and integrated the Fourier function to fit the OpenSim walking simulation data to generate an assistance trajectory that conforms to the ankle joint locomotion law.

We developed a system consisting of high-level, middle-level, low-level controllers, a human and the Ankle-Exosuit system, as seen in Fig. 8. The high-level controller, the outer layer, detects support phase gait events in the gait cycle based on foot plantar pressure sensor measurements. The middle-level controller combines the ankle joint coupling locomotion control model and the OpenSim simulation data to generate the desired position trajectory. The low-level controller, an inner layer, runs closed loop position control on motor position for the actuation system to track the desired cable position trajectories generated by the middle-level controller. The low-level controller controls the value of the output voltage (U_{com}) by correcting the position error (P_{err}), and reduces the error of the Bowden cable output position (P_{cable}) and the desired position

trajectory value (P_{value}). The human and the Ankle-Exosuit control system adjusts the Bowden cable assistance trajectory to assist the locomotion gait of the wearer.

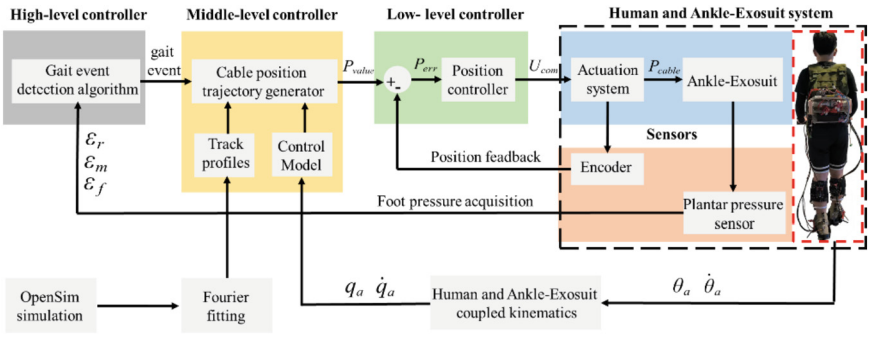

Fig. 8. Schematic block diagram of the Ankle-Exosuit controller. The diagram shows the human and the Ankle-Exosuit system (blue), sensor system (orange), high-level controller (gray), middle-level controller (yellow) and low-level controller (green). The high-level controller completes the gait intention recognition through the threshold detection algorithm, and detects the gait event according to the measured value of the foot pressure sensor. The middle-level control generates the desired assistance trajectory based on the coupling model, trajectory generation function and gait events. The low-level control adjusts the position output of the actuator system to track the desired trajectory generated by the middle-level controller. (Color figure online)

In order to achieve personalized wearing assistance requirements and adapt to different walking gait of wearers, we obtained a gait cycle ankle angle from OpenSim simulation, normalized the coordinates and fitted it to $\theta_{fa}(t)$ by Fourier function, and transformed $\theta_{fa}(t)$ into a generic trajectory generation function by parametric processing.

$$\theta_a(t) = A_a\theta_{fa}\left(\frac{1}{T}t\right) + B_a \tag{7}$$

where $\theta_a(t)$ is the ankle joint angle, A_a is the amplitude, T is the gait period, B_a is the joint angle offset, and $\pm\frac{T}{2}$ is the phase difference between the left and right leg.

According to Eqs. (4) and (7), the model of the ankle joint trajectory generator can be expressed as

$$q_a(t) = \frac{r_a}{R_p}\left(A_a\theta_{fa}\left(\frac{1}{T}t\right) + B_a\right) - \frac{r_a}{R_p}\theta_{a0} + q_{a0} \tag{8}$$

5.2 Trajectory Generator Model Validation

(1) Model parameters calculation

We used the statistical method of sampling to select 10 typical participants from 100 participants with different height and weight, measured and calculated the model parameters, and determined the model parameters by calculating the mean value to increase the accuracy of the model parameters. The model parameters are shown in Table 1.

Table 1. List of model parameters

Symbols	R_p	l_{a0}	r_a	r_c	l_{a1}
Value (mm)	30	180	84	58	192

(2) Model validation

We varied the amplitude A_a, the gait period T and the angular displacement B_a of the ankle joint. In order to verify the trajectory generation function and the locomotion control model, we displayed the joint locomotion trajectories produced by the trajectory generation function across five gait cycles by altering the values of amplitude A_a, gait period T, joint angular displacement B_a of the ankle joint. The locomotion trajectory of the ankle joint was precisely replicated by the trajectory generation function (Fig. 9).

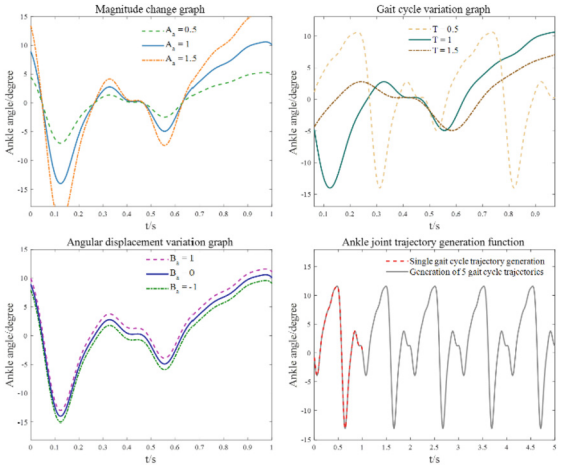

Fig. 9. Verification result of the trajectory generation function

The locomotion trajectory of the input motor was synchronized with the ankle-assisted trajectory (Fig. 10), the rationality of the trajectory generator model was proved..

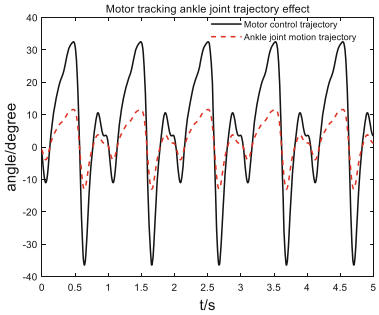

Fig. 10. Angle relationship between Ankle joint and motor.

6 Experiments

In order to evaluate the efficacy of the Ankle-Exosuit, muscle activation is compared unworn the Ankle-Exosuit by the sEMG experiments. A treadmill, a set of sEMG device (Noraxon-DTS series wireless sEMG recording device, USA), and a host computer for data reception (MR23 software) made up most of the experimental apparatus (Fig. 11).

The sEMG assessment experiments included three healthy adult individuals (age = 24 ± 2 years, height = 170 ± 10 cm, weight = 65 ± 10 kg). The two groups of experiments were separated by 10 min to ensure that the muscles could recover sufficiently. Before starting the sEMG experiments, the subjects were informed about the detailed experimental procedure. Six pairs of disposable electrode pads were placed on the surface of six muscles (medial and lateral GM and SM of the left and right legs), which had been previously cleaned with alcohol to allow measurement of the fatigue level of the gastrocnemius and hamstrings muscles. The sEMG acquisition frequency was set to 1500 Hz and the acquisition time was 2 min. The sEMG signal was input to the PC and low-pass filtered, rectified and normalized. We selected the maximum sEMG signal values for 100 gait cycles and summed the GM and HM of the left and right legs to find the mean and standard deviation.

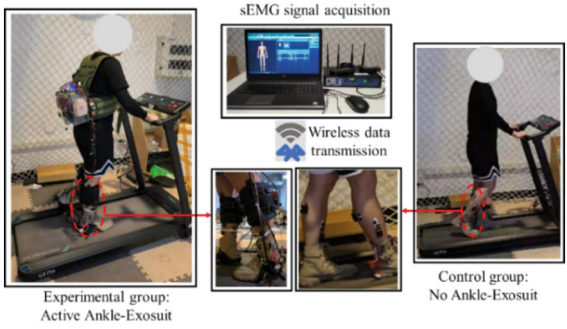

Fig. 11. Subjects wore Ankle-Exosuit with EMG tester for walking test on a treadmill.

The sEMG experiments demonstrated that while wearing the Ankle-Exosuit for ankle gait assistance, the amount of activation of both the GM and SM was reduced, with the GM displaying the most significant performance (Fig. 12). Compared with the unworn the Ankle-Exosuit, the activation rate of the GM muscle and the SM decreased by 11.08% and 6.5%, respectively.

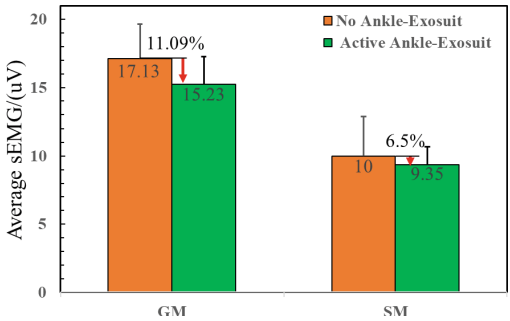

Fig. 12. Comparison of sEMG signals between the experimental and control groups.

7 Conclusion

In this study, we developed an Ankle-Exosuit system to achieve effective walking assistance. A biomimetic Ankle-Exosuit was designed based on the muscle-tendon-ligament model by analyzing biomechanics of the ankle joint. Meanwhile, the bandage locomotion can be effectively reduced by the designed lacing mechanism. The human-exosuit coupled kinematic model was established. Recognition of HO and TO was implemented by threshold detection algorithm. The generation of ankle-assisted trajectory was achieved by the fusion of the coupled kinematic model and trajectory generation function. The Ankle-Exosuit provided assistance to the ankle joint after completing the gait recognition. The assistance trajectory tracking error was reduced by PID feedback control.

Three volunteers participated in the sEMG experiments to assess the auxiliary performance of the Ankle-Exosuit. Comparison experiments demonstrated that when wearing the Ankle-Exosuit, the locomotion activation of the GM and SM decreased by 11.09% and 6.5%, respectively. Conclusively, this comprehensive study indicates that the Ankle-Exosuit system has the ability to reduce muscle activation to enhance human walking endurance, showing great potential to assistance walking in ankle patients with locomotion impairment.

Acknowledgements. This work was funded by Chongqing Science and Technology Commission of China (cstc2020jcyj-msxmX0398), Science and Technology Research Program of Chongqing Municipal Education Commission (KJZD-K202001103, KJQN202201169), the Scientific Research Foundation of Chongqing University of Technology (2019ZD61), and the graduate student Innovation Project of Chongqing (NO. CYS21466). Supported by action plan for quality development of Chongqing University of Technology graduate education (Grant No. gzlcx20233426).

References

1. Olney, S.J., Rsichards, C.: Hemiparetic gait following stroke. Part I: Characteristics. Gait Posture **4**(2), 136–148 (1996)
2. Moriello, C., Finch, L., Mayo, N.E.: Relationship between muscle strength and functional walking capacity among people with stroke. J. Rehabil. Res. Dev. **48**(3), 267–275 (2011)
3. MAili, P., Salvo, F.D., Caserio, M.: Neurorehabilitation in paraplegic patients with an active powered exoskeleton (Ekso). Digit. Med. **2**(4), 163 (2016)
4. Jansen, O., Grasmuecke, D., Meindl, R.C.: Hybrid assistive limb exoskeleton HAL in the rehabilitation of chronic spinal cord injury: proof of concept; the results in 21 patients. World Neurosurg. **110**, e73–e78 (2018)
5. Hong, E., Gorman, P.H., Forrest, G.F.: Mobility skills with exoskeletal-assisted walking in persons with SCI: results from a three center randomized clinical trial. Front. Robot. AI **7** (2020)
6. Milia, P., De Salvo, F., Caserio, M.: Neurorehabilitation in paraplegic patients with an active powered exoskeleton (Ekso). Digit. Med. **2**(4), 163 (2016)
7. Ding, Y., Galiana, I., Asbeck, A..T.: Biomechanical and physiological evaluation of multi-joint assistance with soft exosuits. IEEE Trans. Neural Syst. Rehabilit. Eng. **25**(2), 119–130 (2017)
8. Park, Y.L., Chen, B.R., Perez-arancibia, N.O.: Design and control of a bio-inspired soft wearable robotic device for ankle-foot rehabilitation. Bioinspir. Biomim. **9**(1), 016007 (2014)
9. Wehner, M., Quinlivan, B., Aubin, P.M.: A lightweight soft exosuit for gait assistance. In: Proceedings of the 2013 IEEE International Conference on Robotics and Automation, F, 2013. IEEE (2013)
10. Awad, L.N., Bae, J., O'Donnell, K.: A soft robotic exosuit improves walking in patients after stroke. Sci. Transl. Med. **9**(400), eaai9084 (2017)
11. Schmid, K., Duarte, J.E., Grimmer, M.: The myosuit: bi-articular anti-gravity exosuit that reduces hip extensor activity in sitting transfers. Front. Neurorobot. **11** (2017)
12. Ding, Y., Gallana, I., Siviy, C.: IMU-based iterative control for hip extension assistance with a soft exosuit. In: Proceedings of the 2016 IEEE International Conference on Robotics and Automation (ICRA), F, 2016. IEEE (2016)
13. Lee, G., Ding, Y., Bujanda, I.G.: Improved assistive profile tracking of soft exosuits for walking and jogging with off-board actuation. In: Proceedings of the 2017 IEEE/RSJ International Conference on Intelligent Robots and Systems (IROS), F, 2017. IEEE (2017)
14. Walsh, C.: Human-in-the-loop development of soft wearable robots. Nat. Rev. Mater. (2018)
15. Haxton, H.A.: Absolute muscle force in the ankle flexors of man. J. Physiol. **103**(3), 267–273 (1944)
16. Li, Y.D., Hsiao-Wecksler, E.T.: Gait mode recognition and control for a portable-powered ankle-foot orthosis. Proceedings of the 2013 IEEE 13th International Conference on Rehabilitation Robotics (ICORR), F, 2013. IEEE (2013)
17. Bae, J., De Rossi, S.M.M., O'Donnell, K.: A soft exosuit for patients with stroke: feasibility study with a mobile off-board actuation unit. In: Proceedings of the 2015 IEEE International Conference on Rehabilitation Robotics (ICORR), F, 2015. IEEE (2015)
18. Gallagher, A., Matsuoka, Y., Ang, W,-T.: An efficient real-time human posture tracking algorithm using low-cost inertial and magnetic sensors. In: Proceedings of the 2004 IEEE/RSJ International Conference on Intelligent Robots and Systems (IROS) (IEEE Cat No. 04CH37566), F, 2004. IEEE (2004)
19. Marins, J.L., Yun, X., Bachmann, E.R.: An extended Kalman filter for quaternion-based orientation estimation using MARG sensors. In: Proceedings of the 2001 IEEE/RSJ International Conference on Intelligent Robots and Systems Expanding the Societal Role of Robotics in the the Next Millennium (Cat No 01CH37180), F, 2001. IEEE (2001)

20. Foxlin, E.: Inertial head-tracker sensor fusion by a complementary separate-bias Kalman filter. In: Proceedings of the IEEE 1996 Virtual Reality Annual International Symposium, F, 1996. IEEE (1996)
21. Chevalier, T.L., Hodgins, H., Chockalingam, N.: Plantar pressure measurements using an in-shoe system and a pressure platform: a comparison. Gait Posture **31**(3), 397–399 (2010)